Renewable Energy 146 (2020) 2700–2715

Contents lists available at ScienceDirect

Renewable Energy

journal homepage: www.elsevier.com/locate/renene

The optimal design and operation strategy of renewable energy-CCHP coupled system applied in five building objects

Xingyi Zhu [a], Xiangyan Zhan [a], Hao Liang [c], Xuyue Zheng [a], Yuwei Qiu [a], Jian Lin [a], Jincan Chen [b], Chao Meng [a], Yingru Zhao [a,*]

[a] College of Energy, Xiamen University, Xiamen, 361005, China
[b] Department of Physics, Xiamen University, Xiamen, 361005, China
[c] Center of Science and Technology Industrial Development, Ministry of Housing and Urban –Rural Development, Beijing, 100835, China

ARTICLE INFO

Article history:
Received 17 September 2018
Received in revised form
10 June 2019
Accepted 1 July 2019
Available online 2 July 2019

Keywords:
CCHP coupled with renewable energy
NPV optimization
IRR optimization
MINLP model
Economic and environmental

ABSTRACT

Combined cooling, heating, and power (CCHP) is an economic and eco-friendly technology to mitigate energy issues with remarkable energy efficiency improvement. This study formulates a mixed integer nonlinear programming (MINLP) model for a combined CCHP system coupled with renewable energy, i.e. RCCHP system, which is applied in five different buildings to evaluate the economic and environmental performance under two optimization modes. Net present value (NPV), internal rate of return (IRR) and dynamic payback period (DPP) are introduced as economic indexes, while CO_2 emission reduction rate (CER) is considered as the environmental indicator to determine the optimal combination, capacity, and operation strategies for energy technologies. Results indicate that a combination of electricity purchased at valley period during night with power generated by the combined heating and power (CHP) unit coupled with wind turbine in peak period during daytime is cost-optimal which also enables higher energy efficiency. Meanwhile, the feed-in tariff as well as the uncoordinated electrical and thermal loads both show a significant impact on real-time operation strategies. Compared with the reference separate production (SP) system, the combined system shows better performance when applied to shopping mall under both optimization modes, e.g., with NPV up to 67.65 and 46.61 million RMB, IRR up to 20.70% and 25.10%, and the minimum DPP is 5.49 and 4.82 years under NPV and IRR maximization, respectively.

1. Introduction

Currently, environmental crisis like the overwhelming smog with frequent occurrence has forced extensive concerns that energy consumption structure for social development expects transformation urgently. However, fossil fuel remains the dominant energy source in Chinese energy consumption [1], and full-fledged mineral energy power generations equipped with large capacity can be operated with observably stability, which contributes a paradox that there are flourishing social economic activities accompanied by a healthy living environment. Therefore, clean renewable energy sources, characterized with low energy waste and low pollution emission, are considered as a supplement or substitute of the traditional fuel.

Against that backdrop, distributed energy resources (DERs) comprised of natural gas (NG), solar energy, wind energy and other renewable resources famous for inexhaustibility, pure cleanliness, etc. are increasingly important for social energy consumption [2]. Meanwhile, the CCHP system as representative integrated production system has been proved to be a valid method to achieve economic benefits, energy saving, and CO_2 emission reduction [3]. How to take all advantages of DERs to inspire CCHP system and choose appropriate performance indexes for the optimization of CCHP system, according to the complementary characteristics of different energy sources as well as reasonable coordination and cooperation in the production of secondary energy [4], makes great sense to the implementation of economic benefits and environmental protection [5].

In this context, a number of researches in literature have investigated the CCHP system, which involve system construction, operation strategy and performance assessment [6–8]. For example, Rahman et al. [9] proposed an exhaustive review introducing kinds of integrated CCHP energy systems and the operation and control strategies of integrated distributed energy resources. As for system construction, Sepehr et al. [10] constructed a CCHP system depending on both natural gas and solar energy import,

* Corresponding author.
E-mail address: yrzhao@xmu.edu.cn (Y. Zhao).

https://doi.org/10.1016/j.renene.2019.07.011
0960-1481/

where the two subsystems exist simultaneously, namely the solar collection subsystem and the CCHP subsystem. Wu et al. [11] built a comprehensive micro-CCHP system, equipping with various components including gas engine, adsorption chiller, electric chiller, auxiliary devices, and etc. Facci et al. [12] reported an example of a complex tri-generation plant where gas turbines and reciprocating engines are involved in as tri-generative (i.e. electricity, thermal and cooling) systems. The established CCHP system could employ various energy inputs such as natural gas, wind energy, solar energy and biomass, while the type of driven energy input does give a significant contribution in structure construction of the CCHP system.

The majority of the research on operation strategies of a CCHP system can be summarized as following the electrical load (FEL) model [13] and following the thermal load (FTL) model [14] as well as some other chosen operation strategies. In terms of the FEL strategy, the combined heating and power (CHP) is determined according to electricity demand, which means that the proportion of waste heat exhausted from CHP can be calculated according to its electricity supply, and the rest thermal demand can be satisfied by auxiliary heating devices [15]. While in the FTL mode, power generation is determined by thermal and cooling load so as to guarantee enough recovered waste heat and the insufficient electric energy will be imported from public grid [16]. Overall, the FEL, FTL and some other multi-objective optimization strategies laid the foundation for the CCHP system operation [17–21].

Studies on the evaluation of CCHP systems have achieved the performance evaluation based on kinds of optimization modes [22,23]. Some previous researches [24,25] applied Life Cycle Assessment (LCA) methodology to promote the environmental, economic, and energy performance for the CCHP system. Nosrat et al. [26] applied PVTOM (PV trigeneration optimization model) to representative buildings located in Canadian regions to evaluate the energy utilization efficiency and carbon emission reduction. Cho et al. [27] optimized the operation of CCHP systems by taking into account the operation cost, carbon dioxide emissions and primary energy consumption.

As mentioned above, there are studies currently focused on the optimal design, operation strategy and performance evaluation of CCHP systems from different perspectives. However, most of those studies do not consider the prime mover design and the variation of load characteristic of different building objects simultaneously, in which the type and performance of prime mover are always designated artificially. Hence, it may not be the optimal result with the empirical hypothesis and limited by the energy production of gas engine or gas turbine which can be significantly influenced by diversified energy requirements of buildings. Meanwhile, the limitation directly impacts design capacity, technology combination and system performance. Moreover, most researches formulate the technology production through simply multiplying the input energy by a fixed efficiency and take no account into how the load fluctuation will impact the part load operation of prime mover, which is not conducive to improve the accuracy of simulation models. Besides, few researches have ever applied a CCHP system coupled with wind power to design the supply side technology combination and hourly operation strategy for different urban functional buildings differing in size and energy requirements.

Therefore, this study formulates a comprehensive mixed integer nonlinear programming (MINLP) modeling framework to optimize the technology combination, design capacity, and hourly operation strategy of the RCCHP system. Meanwhile, a numerical case study for the planning of five different urban functional buildings characterized by various energy demand is presented to demonstrate the effectiveness and superiority of the proposed method. Unlike most of the existing studies using linear black box models which ignore the influence of load fluctuation and operating load on the efficiency of main energy supply devices, dynamic efficiency by curve fitting under hourly load and off-design condition is considered in this paper. Moreover, multiple auxiliary devices are integrated and optimized to improve the overall performance of the system, such as renewable energy generators like wind turbine and PV panels, energy storage systems as well as boilers and cooling chillers. Besides, preferential policies like carbon tax and electricity feed-in tariff are both involved in this research to realize the economic and environmental benefits of the RCCHP system. Specifically, a 15-year planning horizon with 1440 time intervals (15 years $\times$ 4 seasons $\times$ 24 daily hour periods) is selected in the two optimization cases to ensure accuracy.

The rest of this paper is organized as follows. Section 2 describes the structure of the RCCHP system including combined heating and power subsystem (CHP subsystem) as prime mover, renewable subsystem, and auxiliary energy subsystem. Section 3 takes the reference system for comparison and introduces environment, economic, and energy performance indexes. Section 4 proposes an original objective operation optimization model with multiple integers and non-linear variables for the RCCHP system under NPV optimization (NOM) objective functions and IRR optimization (ROM) objective functions. Section 5 introduces five different buildings characterized by different energy demand profiles, followed by analysis and evaluation of the optimized results under the two objective functions. Finally, primary conclusions and prospects are given in Section 6.

2. Problem description

As mentioned in introduction, both supply side technologies and demand side response are taken into account in the RCCHP system model. Supply side technologies are comprised of distributed energy conversion technologies and centralized energy conversion technologies. In terms of a feasible RCCHP site, a certain number of CHP units, renewable energy conversion units, accessory power devices, auxiliary heating units and cooling equipped components are absolutely indispensable. Aforementioned system structure can be optimally designed so as to excellently compensate energy consumption balance. Furthermore, each RCCHP site can exchange electric power with public grid (PG) connected by an electrical interface. The surplus electricity produced by the CHP units and/or renewable energy devices is sold back to PG, meanwhile it is possible to import electricity from the grid when the electrical demand exceeds production. To coordinate demand side supplement balances and supply side conversion configurations at the same time, it is far from reliability to rely solely on conventional design disciplines and traditional operational strategies. The RCCHP system model proposes optimal energy flow and capacity allocating issue with an energy systems optimization program based on advanced digitization. The system superstructure described by the RCCHP energy model is shown in Fig. 1, in which the supply side can be equipped with a CHP unit choosing a gas turbine (GT) or a gas engine (GE). Solar photovoltaic generators (PV) and wind turbines (WT) are introduced as the other two clean renewable energy resources. Heat recovery steam generator (HRSG), electric boiler (EB), and thermal storage tank (TST) provide thermal energy. LiBr absorption chiller (ABS) and electric chiller (EC) are employed to undertake the overall cooling load. In Fig. 1, the green, blue, and red lines are defined to represent electricity, cooling, and thermal flows respectively, while the black line indicates natural gas flow. The RCCHP system can be applied to diverse locations by changing the input value which illustrates the technical configurations and the demand-side load. The following information is prerequisites for the optimization:

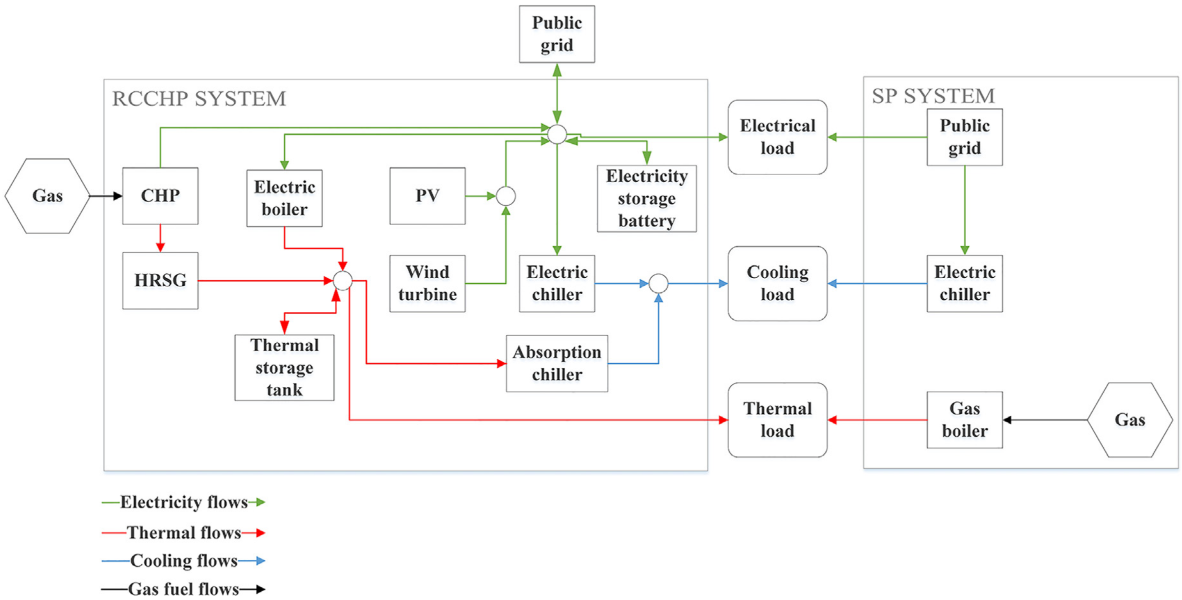

Fig. 1. The schematic diagram of RCCHP and SP systems driven by natural gas and renewable energy.

- The hourly electrical, thermal, and cooling load profiles for a typical day of the four seasons in five different buildings over the entire time horizon;
- The real-time solar irradiance profile and the hourly wind speed profile in the height of wind turbine hub for four typical days of the introduced buildings;
- The technical performance data related to the CHP units, renewable devices, auxiliary thermal technologies, kinds of chillers and energy storage devices;
- The initial investment and maintenance costs at the prevailing market level and the carbon tax from the up to date policy;
- The feed-in tariff and time-of-use electricity tariff;
- The natural gas purchasing price.

So as to address the design and planning problem of integrated energy system for demand side with the purpose of economic benefit, environmental benefit and social benefit, the proposed model aims at maximizing NPV or IRR, both of which calculate initial investment costs, yearly operation and maintenance costs as well as environmental carbon tax expenditure. A series of building objects comprised of office, hotel, residential, hospital and shopping mall are selected as optimization cases. After the optimized simulation the collection of energy conversion technologies will be allocated appropriately to better serve the local energy consumption, as a result the integration and operation of technologies will be improved. The optimization model is then applied to a time horizon constituted by the set of selected typical days of each season. Fig. 2 indicates the basic structure of the RCCHP system. The main outputs of the optimal model are:

- Existence and size of CHP components;
- Existence and number of renewable conversion devices;
- Electricity yielded by both CHP units and renewable conversion devices;
- Primary energy consumption and CO_2 emission by each chosen CHP unit;
- Electricity, thermal and cooling flow through junction inside the RCCHP system network;
- Optimal operation strategy and operation status of all energy devices in each time interval.

Furthermore, the RCCHP model finally comes out three performance indexes of energy, economy, and environment. The total operation cost (TOC) and environment-friendly carbon taxes in the annual cycle are conducive to annual NPV, IRR, and DPP calculation. The CER is presented to be an indicator of environmental assessment during the optimal procedure. Finally, combined efficiency for energy utilization is an indispensable factor to quantify the distributed energy saving due to the operation of RCCHP systems compared with the reference system producing electricity and heating separately.

3. Operation performance evaluation indexes

3.1. Reference system

To carry out the analysis, a reference SP is proposed with a definite physical structure that consists of gas boiler and electric chiller as well as the public grid as shown in Fig. 1.

3.2. Indexes

Since the related expense of renewable conversion devices is proverbially higher than that of traditional energy resources and the CO_2 emission factor is rather lower, performance indexes of energy, economy and environment should be taken integrally into overall consideration.

3.2.1. Environmental performance indexes

Environmental impact is an unavoidable problem in energy system design. With international attention to carbon dioxide emissions, the equivalent CO_2 emission generated by the RCCHP system, the CCHP system, and the SP system are all considered. CER as the environmental performance index is the basis of carbon tax calculation, which can be detailed as

$$CE^{SP} = \sum_s \sum_t \left(\alpha^{ng} \cdot GC_{s,t}^{SP} + \alpha^{el} \cdot EIG_{s,t}^{SP} \right) \tag{1}$$

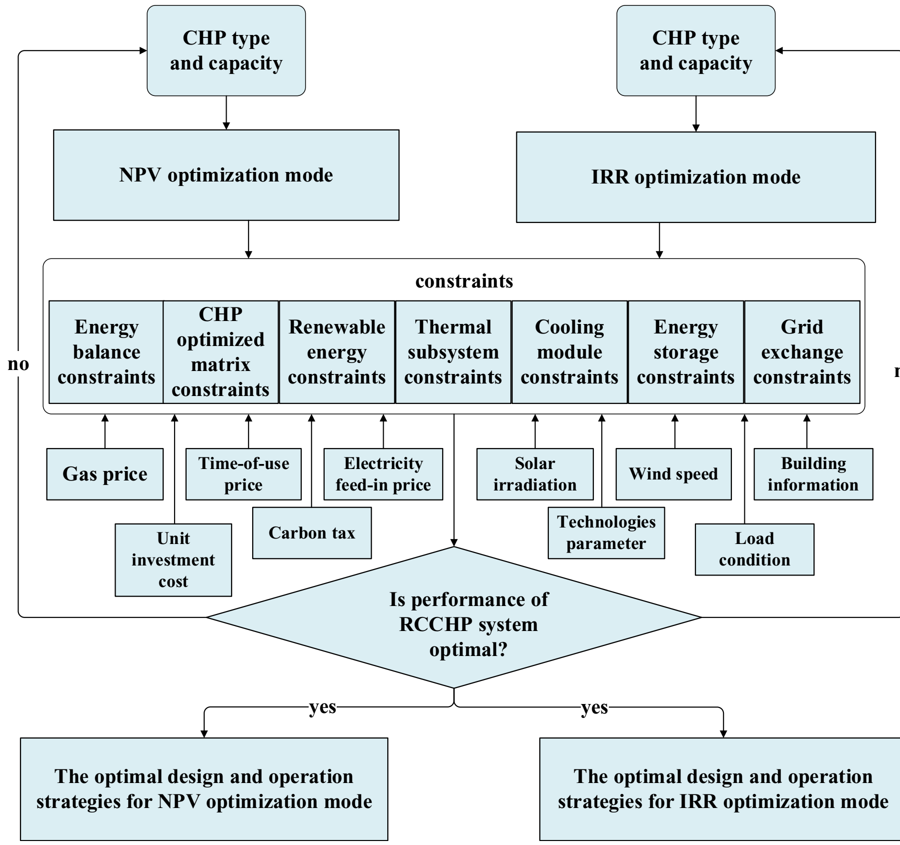

Fig. 2. Basic structure of RCCHP system.

$$CE^{RCCHP} = \sum_s \sum_t \left(\alpha^{ng} \cdot GC_{s,t}^{RCCHP} + \alpha^{el} \cdot EIG_{s,t}^{RCCHP} \right) \tag{2}$$

$$CER^{RCCHP} = \frac{CE^{SP} - CE^{RCCHP}}{CE^{SP}} \tag{3}$$

where carbon emission CE, gas consumption GC and electricity are imported from the public grid EIG, all of which are dependent on the operating schedule of supply side technologies and the load level of demand side. α^{ng} and α^{el} represent the carbon emission factor of kilowatt natural gas consumption 220 g/kWh in the RCCHP system and kilowatt electric power 968 g/kWh imported from the public grid, respectively. The superscript ng and el here stand for natural gas and electric energy. The subscript s and t represent seasons and hours, respectively.

3.2.2. Economic performance index

Initial investment cost (IIC), total operation cost (TOC), NPV, IRR, and DPP calculated in this paper collectively reveal the economic performance for the RCCHP system.

The total operation cost (TOC)

For the RCCHP system, the yearly TOC accumulates electricity purchasing cost from PG, negative electricity selling income, total NG consumption cost are calculated by

$$TOC^{RCCHP} = 90 \cdot \sum_s \sum_t \left(\gamma_{s,t} \cdot EIG_{s,t}^{RCCHP} - \sum_{ec} \left(\lambda^{ec} \cdot ESG_{s,t}^{ec} \right) + \mu^{ng} \cdot GC_{s,t}^{RCCHP} \right) + \sum_c (pm_c \cdot EO_c) + 90 \cdot \varphi \cdot CE^{RCCHP} \tag{4}$$

For SP system, the yearly TOC can be represented as

$$TOC^{SP} = 90 \cdot \left(\sum_s \sum_t \left(\gamma_{s,t} \cdot \left(EL_{s,t} + CL_{s,t} \cdot \frac{1}{COP^{EC}} \right) + \mu^{ng} \cdot GC_{s,t}^{SP} \right) + \varphi \cdot CE^{SP} \right) \tag{5}$$

where γ is time-of-use price for electricity purchased from PG, μ is natural gas price and pm is the maintenance cost factor. Note that λ indicates electricity feed-in tariff for introduced electricity generators ec, and φ is the unit price of carbon tax 300 ¥/ton. There are two new variables in Eq. (4), electricity sold back to PG associated with per electricity power generator ESG and timely electricity purchasing from public grid EIG. Besides, EL and CL in Eq. (5) represent the electrical load and cooling load, respectively. It is of more realistic significance to adopt different electricity feed-in tariff λ multiplied by ESG to calculate interconnection benefits. Besides, COP^{EC} in Eq. (5) is related to the coefficient of performance of electric chiller.

The RCCHP system coupled with renewable conversion devices and energy storage system could account for gas consumption reduction of CCHP system. The saving cost SC can be identified as incremental benefits of the RCCHP system, given as follows

$$SC = TOC^{SP} - TOC^{RCCHP} \tag{6}$$

The initial investment cost (IIC)

The IIC refers to the initial investment cost calculated by multiplying unit cost factor by rated capacity, which can be formulated by

$$IIC^{RCCHP} = \sum_{c}(pi^{c} \cdot TR^{tc}) + \sum_{c}(pi^{c} \cdot CR^{cc}) + \sum_{c}(pi^{c} \cdot ER^{ec}) \tag{7}$$

$$IIC^{SP} = \sum_{c}(pi^{c} \cdot (TR^{tc} + CR^{cc})) \tag{8}$$

where pi is the cost per unit of capacity of allocated techniques, which is associated with the sorts of allocated energy technologies c. In addition, other superscripts tc, ec, and cc present to be a subset of c which indicate thermal supply technologies, electricity output technologies and cooling supply technologies, respectively. What is worth mentioning is that this research regards WT, PV and CHP as electricity output technology ec, and TST and electric boiler EB as thermal supply technologies tc in the RCCHP system. Here, ER, TR and CR represent the rated capacity allocation associated with ec, tc and cc, respectively. The rated capacity of all devices is a variable of system optimization and particularly the capacity of prime mover is optimized selection from GE categories and GT categories. What's more, the ER of WT and PV is well correlated with the allocated number.

The net present value (NPV) and internal rate of return (IRR)

It is known that the RCCHP system has relative economic advantages in terms of operating expenses, but efficient and economical system always means higher initial investment cost [9]. In addition, the RCCHP system generates benefits by reducing operation cost and carbon tax reduction, but its adoption makes an incremental installation cost. Therefore, the simple accumulation of the IIC and the TOC is insufficient for the optimization. In this paper, the RCCHP system is optimized by using the NPV or the IRR as the target function, described by

$$NPV = \sum_{y=1}^{T} SC_{y} \cdot (1+i)^{-y} - \left(IIC^{RCCHP} - IIC^{SP}\right) \tag{9}$$

where i and y represent the discount rate for 6%, the operation time period lasts for 15 years. And the IRR can be formulated as

$$\sum_{y=1}^{T} SC_{y} \cdot (1+IRR)^{-y} - \left(IIC^{RCCHP} - IIC^{SP}\right) = 0 \tag{10}$$

Noted that the IRR represents the yield rate when all investments happen to be recovered and the project is winding up, which mainly reflects the expected payback rate of the project investment. Only when the IRR is higher than the expected payback rate, the investment project is feasible. Therefore, the higher the IRR is, the smaller the investment risk and the better the feasibility for an investment project.

The dynamic payback period (DPP)

The DPP is capital recover time when NPV is equal to 0 [28]. The smaller the DPP value is, the faster the capital recovery speed so that the project plan is a better choice for decision maker. The DPP is formulated as

$$\sum_{y=1}^{DPP} SC_{y} \cdot (1+i)^{-y} - \left(IIC^{RCCHP} - IIC^{SP}\right) = 0 \tag{11}$$

3.2.3. Energy performance indexes

For the RCCHP system, the energy utilization rate (EUR) could be calculated by

$$EUR^{RCCHP} = \frac{\sum_{s}\sum_{t}(TL_{s,t} + EL_{s,t} + CL_{s,t})}{\sum_{s}\sum_{t}\left(GC_{s,t}^{RCCHP} + EO_{s,t}^{WT} + EO_{s,t}^{PV} + \frac{EIG_{s,t}^{RCCHP}}{(0.4COP^{PG})}\right)} \tag{12}$$

where COP^{PG} is transmission efficiency based on the average level of the local PG and the specific value 0.4 is the conversion efficiency of the bidding coal from grid statistics [29]. Similarly, TL in the above two equations is real-time thermal load. EO in Eq. (12) refers to the electricity produced by WT and PV.

On account of the renewable energy conversions, gas saving rate (GSR) could be a relevant parameter to reveal the contribution by WT and PV when it comes to energy performance for the RCCHP system [30], which can be illustrated by

$$GSR_{s}^{RCCHP} = \frac{\sum_{t}\left(GC_{s,t}^{SP} - GC_{s,t}^{RCCHP}\right)}{\sum_{t}\left(GC_{s,t}^{CCHP}\right)} \tag{13}$$

4. Mathematical model description

The model proposed in this paper will help to address the following question: five kinds of planning areas comprised of office, hotel, hospital, residential building and shopping mall with its certain renewable resources, available surrounding conditions and energy consumption profiles, where the collection of energy conversion technologies will be allocated appropriately to serve the local energy consumption better and how these technologies will be integrated and operated. The optimization model is then applied to a time horizon constituted by a set of selected typical days.

A MINLP (mixed-integer nonlinear programming) model is therefore formulated in GAMS 2.5 employing the Lindo optimizer for seeking the optimal allocation of RCCHP system. The objective function of the model is to maximize NPV, whose main decision variables refer to the type, size, combination, and operating strategy of the technologies, which will be described in Section 4.1. Unlike the previous studies where the CHP types and sizes were preassigned factitiously for specific planning areas and the coupled renewable energy devices are not optimized for quantities under different feed-in tariffs, the different CHP schemes for different optimization areas are considered in the present model, where the real separated sale prices of WT and PV are serving as a new parameter for renewable energy allocation.

4.1. The objective function

The NPV and IRR in this paper play a critical role in the RCCHP system distinguished from previous researches for kinds of destination areas. The total cost minimization of distributed energy system over a time horizon is not an easy task due to the complex optimization of supply side technologies. Apparently, lower operation cost means that the system could operate with little business expenses for better economic performance and lower CER means that the system operates with large amount of CO_2 emission reduction for better environmental performance. Therefore, how to coordinate the relationship between economic and environment is the main optimization objective for the RCCHP system. The NPV introduced in this paper including initial installation, operation cost and environment-friendly carbon taxes in the designed life cycle is to achieve the optimal economic benefits and environmental benefits of RCCHP system on the premise of satisfying the fluctuant energy demand. While the IRR in this research is organized to combine the total economic benefits during the operation time period with the initial investment cost. The optimal IRR can be compared with benchmark investment rate so that it can be found out whether the project is worth investing in. Note that NPV and IRR are identified as the integration criterion best suited for optimization, and the objective function is examined for a multi-year period. The detailed objective functions are described in Eq. (14) and Eq. (15). Note that the equation of the IRR is not an explicit function.

$$\max NPV = \sum_{y=1}^{T} SC_y \cdot (1+i)^{-y} - \left(IIC^{RCCHP} - IIC^{SP}\right) \tag{14}$$

$$\begin{cases} \sum_{y=1}^{T} SC_y \cdot (1+IRR)^{-y} - \left(IIC^{RCCHP} - IIC^{SP}\right) = 0 \\ \max\ IRR \end{cases} \tag{15}$$

4.2. Constraint conditions

In the MINLP optimization model, based on energy supply balance and energy conversion rule, constraints are divided into three main different types: energy balance constraints, technology conversion constraints and network exchange constraints.

4.2.1. Energy balance constraints

Energy balance constraints are formulated to impose restrictions on the electricity, thermal and cooling power flow equilibrium for each node in each time interval.

The supply and demand of electricity in RCCHP system are expressed as

$$ES_{s,t} + EO_{s,t}^{ESB} + EIG_{s,t} = EI_{s,t}^{EC} + EI_{s,t}^{EB} + EI_{s,t}^{ESB} + EI_{s,t}^{TST} + EL_{s,t} \tag{16}$$

where EI refers to the electricity input for electricity consumption equipment and EO is the real-time discharge power of electric storage battery. Note that ES represents the total electricity production subtracted the total electricity sold back to PG, which will be described in detail in the subsequent grid exchange constrains.

The total thermal and cooling energy production from supply side technologies must be equal to the sum of corresponding energy loads from demand side and specific technology dissipation (such as the thermal energy fed in ABS). The supply and demand of thermal and cooling energy in the RCCHP system are expressed as

$$TO_{s,t}^{HRSG} + TO_{s,t}^{EB} + TO_{s,t}^{TST} \geq TI_{s,t}^{ABS} + TI_{s,t}^{TST} + TL_{s,t} \tag{17}$$

$$CO_{s,t}^{ABS} + CO_{s,t}^{EC} \geq CL_{s,t} \tag{18}$$

where TO means the thermal output from the thermal supply devices and TI is the thermal energy fed in thermal consumption devices. Similarly, CO in Eq. (18) is cooling energy produced by cooling chillers.

4.2.2. Technology conversion constraints

The CHP optimized matrix constraint

In this research, the CHP types and sizes are not preassigned factitiously for specific planning areas which are characterized by significant heat-to-power ratio difference for energy demands with different fluctuation level. A gas turbine or a gas engine choice closely depends on energy consumption situation due to the difference of thermal-electrical efficiency. For example, the gas engine with higher electricity-production ability presents to be with much stronger compatibility for a local area equipped with relatively lower heat-to-power ratio in an overall level. Therefore, a binary integer variable matrix is constructed for the optimal choice of the CHP types and sizes in Eq. (19). Then, kinds of gas engines and gas turbines with specific capacity are introduced based on the hourly energy consumption of the five planning objective areas under investigation. A CHP module integrated with gas engines and gas turbines is described mathematically for electricity and thermal energy production. The detailed relative functions are described by

$$x_m^{CHP} = \begin{bmatrix} x_1^{GT} & x_2^{GT} & x_3^{GT} & x_4^{GT} \\ x_1^{GE} & x_2^{GE} & x_3^{GE} & x_4^{GE} \end{bmatrix} \tag{19}$$

$$EO_{m,s,t}^{CHP} = \begin{bmatrix} EO_{1,s,t}^{GT} & EO_{2,s,t}^{GT} & EO_{3,s,t}^{GT} & EO_{4,s,t}^{GT} \\ EO_{1,s,t}^{GE} & EO_{2,s,t}^{GE} & EO_{3,s,t}^{GE} & EO_{4,s,t}^{GE} \end{bmatrix} \tag{20}$$

$$EO_{m,s,t}^{CHP} = x_m^{CHP} \cdot GC_{m,s,t}^{CHP} \cdot COPel_{m,s,t}^{CHP} \tag{21}$$

$$\sum_{GT} x_m^{GT} + \sum_{GE} x_m^{GE} = 1 \tag{22}$$

$$f_{m,s,t}^{CHP} = \frac{EO_{m,s,t}^{CHP}}{ER^{CHP}} \tag{23}$$

$$COPel_{m,s,t}^{CHP} = a_1^{CHP} \cdot \left(f_{m,s,t}^{CHP}\right)^2 + a_2^{CHP} \cdot f_{m,s,t}^{CHP} + a_3^{CHP} \tag{24}$$

$$cut^{CHP} \cdot ER^{CUP} \leq EO_{m,s,t}^{CHP} \leq ER^{CHP} \tag{25}$$

$$TO_{m,s,t}^{CHP} = x_m^{CHP} \cdot GC_{m,s,t}^{CHP} \cdot COPth_{m,s,t}^{CHP} \tag{26}$$

$$COPth_{m,s,t}^{CHP} = b_1^{CHP} \cdot \left(f_{m,s,t}^{CHP}\right)^2 + b_2^{CHP} \cdot f_{m,s,t}^{CHP} + b_3^{CHP} \tag{27}$$

where x is the binary variable standing for the existence of the CHP with different capacity. The CHP in this research involves in gas engine and gas turbine allocated with different capacities. Eq. (22) represents only one type of the CHP decision with specific capacity. f in Eq. (23) is the part load factor which is obtained by dividing real-time electricity output from the chosen CHP EO by the rated power ER. Here, $COPel$ and $COPth$ refers to the hourly electrical efficiency and thermal efficiency which are both associated with the part load factor f. Therefore, partial-load efficiency curves for electricity and thermal energy production are fitted as quadratic nonlinear equation with three described coefficients a_1, a_2, a_3 or b_1, b_2, b_3, respectively. The production of the CHP should not exceed rated power ceiling and the floor level limited by cut-out coefficient cut to avoid overload or underload condition.

Renewable energy constraints

Two feasible renewable technology choices are introduced in this model, i.e., PV systems and WT devices. Available natural renewable energies are under particular investigation located in the planning target areas in this paper. Technical characteristic and market price serve as the input parameters for renewable technology optimization.

The output power of a PV device is related to installation inclination, solar radiation quantity, dust cover, and ambient temperature. This paper adopts a simplified PV system model. Under the premise of the optimum tilt Angle setting, electricity production by the PV system is proportional to local solar radiation and ambient temperature embodied in a nonlinear mathematical model, where the hourly solar radiation values in four typical days of four seasons are taken as input values. The output power of the PV system can be calculated by

$$EO_{s,t}^{PV} = COP^{PV} \times W_{s,t} \times num^{PV} \times A^{PV} \tag{28}$$

$$0 \le num^{PV} \cdot A^{PV} \le TA^{PV} \tag{29}$$

where *EO* refers to the electric energy output from PV devices, *num* represents the installed number of the PV which is a variable to be optimized. *W* (J/m2) presents to be time-related solar irradiation in the corresponding location and the parameter COP^{PV} is the efficiency taken as a constant that equals to 14.2%. Besides, *A* and *TA* are two parameters representing the average size of a PV panel and the available allocated space respectively. The allocation number of PV *num* is conditioned by the available space *TA*.

Wind power production is proportional to the vertical of wind speed for specific WT type. Normally, the available active power generation imported from wind energy at a variable speed WT is identified as

$$EO_{s,t}^{WT} = \begin{cases} num^{WT} \cdot 0 \; v_{s,t} < v^{in}, v_{s,t} > v^{out} \\ num^{WT} \cdot \left(c_1 \cdot v_{s,t}^3 + c_2 \cdot v_{s,t}^2 + c_3 \cdot v_{s,t} + c_4 \right) v^{in} \le v_{s,t} < v^{rated} \\ num^{WT} \cdot ER^{WT} \; v^{rated} \le v_{s,t} \le v^{out} \end{cases} \tag{30}$$

where *EO* represents the electric energy output from WT devices, *num* is the allocated number of WT which is a variable to be optimized. Besides, v^{in}, v^{rated} and v^{out} are cut in wind speed, rated wind speed and cut out wind speed, respectively. Wind power generation is tightly associated with real-time wind speed *v* according to the power-wind-speed curve which is given by manufacturers. The power curve is fitted as nonlinear cubic mathematical equation with four certain parameters, i.e. c_1, c_2, c_3 and c_4.

A variable-pitch variable-speed WT holds the optimal *Cp* ($=Cp_{max}$) to chase the maximum power output by controlling the rotor speed. Then it operates at the max rotor speed with wind speed increasing continuously until the realization of rated power production. From the rated wind speed to the exceed wind speed, the constrain of generator speed WT maintains the rated power regulation by varying the pitch angle.

Auxiliary thermal subsystem constraints

The CHP unit undertakes the production of electricity and thermal energy simultaneously. However, asynchronous consumption of electrical power and thermal energy makes it necessary for the allocation of the auxiliary thermal subsystem.

The HRSG in the RCCHP system is a recovery device which recycles waste thermal by-product of CHP units to provide the thermal energy fed in ABS and heating heat loss of demand side. The mathematical model is shown by

$$TO_{s,t}^{HRSG} = TI_{s,t}^{HRSG} \cdot COP^{HRSG} \tag{31}$$

$$TO_{s,t}^{HRSG} \le TR^{HRSG} \tag{32}$$

where *TI* is the thermal input of HRSG subsystem which is recovered by the waste heat exhausted from CHP generators. The HRSG plays an important role in energy gradient utilization. And, *TO* as the thermal output from recovery waste heat is prepared for the thermal energy load of demand side and the thermal consumption of ABS for chilling. Besides, TR here represents the optimal capacity of the HRSG subsystem.

The existence of electric boiler is to produce extra thermal so that when a CHP is not in full load operation condition the unreasonable decline of thermal deficiency can be avoidable. The mathematical model of electric boiler is shown by

$$TO_{s,t}^{EB} = EI_{s,t}^{EB} \cdot COP^{EB} \tag{33}$$

$$TO_{s,t}^{EB} \le TR^{EB} \tag{34}$$

Cooling module constrains

Based on the gradient utilization, the thermal energy generated by CHP units and electric boiler or discharged by thermal storage tank is delivered to the absorption chiller for cooling energy production. The coefficient of performance (COP^{ABS}) is introduced to illustrate the energy conversion efficiency. Eqs. (35) and (36) show the production of ABS, illustrated by

$$CO_{s,t}^{ABS} = TI_{s,t}^{ABS} \cdot COP^{ABS} \tag{35}$$

$$CO_{s,t}^{ABS} \le CR^{ABS} \tag{36}$$

where *CO* represents the cooling energy output from absorption chiller, *TI* represents the thermal consumption associated with the cooling energy production. Besides, *CR* is the optimal rated capacity of absorption chiller. There is an inequality constraint in Eq. (36) which illustrates the production ceiling.

Since the on or off state of absorption chiller is totally dependent on the production of thermal energy by CHP units, an electricity-driven chiller is indispensable when the real-time cooling load exceed the load capacity of absorption chiller. Electric chiller adopts a similar coefficient for steady running condition. Eqs. (37) and (38) show the boundary limits for electric chiller, i.e.,

$$CO_{s,t}^{EC} = EI_{s,t}^{EC} \cdot COP_{EC} \tag{37}$$

$$CO_{s,t}^{EC} \le CR^{EC} \tag{38}$$

Energy storage constrains

Volatility and uncertainty of the RCCHP system coupled with renewable energy devices call for electricity and thermal storage modules to address the surplus energy. Thermal storage tank and electricity storage battery are allocated to store the excess energy in order to increase the operational flexibility and reliability. When storage switches on, it is defined as operating in one of the following three states:

- state of being stored;
- state of being charged;
- state of being discharged.

The three-state mathematical models of two energy storage settings in this paper give a detailed description about the charging, discharging and stored situation as well as some boundary constrains.

$$E_{s,t}^{ESB} = E_{s,t-1}^{ESB} + EI_{s,t}^{ESB} - EO_{s,t}^{ESB} - ELS_{s,t}^{ESB} \tag{39}$$

$$EI_{s,t}^{ESB} \cdot EO_{s,t}^{ESB} = 0 \tag{40}$$

$$T_{s,t}^{TST} = T_{s,t-1}^{TST} + TI_{s,t}^{TST} - TO_{s,t}^{TST} - TLS_{s,t}^{TST} \tag{41}$$

$$TI_{s,t}^{TST} \cdot TO_{s,t}^{TST} = 0 \tag{42}$$

where $E_{s,t}$ and $T_{s,t}$ represent the current electricity storage and thermal energy storage quantity, respectively. $E_{s,t-1}$ and $T_{s,t-1}$ stand for the last-moment electricity storage and thermal energy storage quantity before charging and discharging action in this current operation interval, respectively. Electricity charging EI^{ESB} and Electricity discharging EO^{ESB} should not happen at once, while thermal storage TI^{TST} and thermal consumption TO^{TST} should not occur at the same operation step which is detailed in Eq. (39) and Eq. (42). Besides, *ELS* and *TLS* are the electricity loss and thermal energy loss, respectively.

4.2.3. Grid exchange constrains

As mentioned above, the RCCHP site simulated in this research could exchange electricity with PG by an electrical interface. The surplus electricity produced by the CHP and/or the renewable energy device is sold to the distribution grid at different prices, meanwhile it is possible to import electricity from the grid when electrical demand of the district goes beyond the total yield of RCCHP systems. The logic relation of electricity transaction is explicitly illustrated by

$$EIG_{s,t} \cdot EI_{s,t}^{ESB} = 0 \tag{43}$$

$$ESG_{s,t}^{ec} + ES_{s,t}^{ec} = EO_{s,t}^{ec} \tag{44}$$

$$ES_{s,t} = \sum_{EC} ES_{s,t}^{ec} \tag{45}$$

$$EIG_{s,t} \cdot ESG_{s,t}^{ec} = 0 \tag{46}$$

where *ES* means the rest of electricity output by each power generator *ec* deducting the electricity sold back to distributed grid. Note that electricity purchasing *EIG* and electricity storing *EI* cannot happen at the same time. Similarly, the electricity purchasing for the RCCHP system *EIG* and electricity selling from power generator *ec ESG* cannot happen at the same time as well.

5. Case study and discussion

In order to comparatively analyze and evaluate the combination and operation performance of the RCCHP and SP systems, this paper selects five building objects of the innovation pilot zone in Shanghai, China. Shanghai belongs to the tropical monsoon climate of the northern subtropical zone which is characterized by four distinctive seasons with rainfall and abundant sunshine, for which the technical parameters and economic parameters are illustrated in Table 1 and Table 2, respectively. Besides, parameters of energy price of the RCCHP system are detailed in Table 3.

5.1. Energy demand profiles

Overall, humid and mild Shanghai turns out to possess favorable natural energy sources. This research draws a group of residential, office, hospital, hotel and shopping mall. The five clear energy loads profiles of the buildings along with its corresponding heat-to-power ratio are illustrated in Fig. 3, and the peak load values of the buildings are shown in Table 4. In Fig. 3, electricity, thermal and cooling load for 24 h of a typical day in four seasons are displayed, abbreviated to *spr*, *sum*, *aut* and *win*, respectively.

The heat-to-power ratio (HTP) of the annual loads of the buildings contributes a significant influence on the energy system performance, illustrated by

Table 1
Technical parameters values for SP and RCCHP system [10,21,25].

system	technology	parameter	value
SP	PG	COP^{PG}	0.920
	GB	COP^{GB}	0.880
	EC	COP^{EC}	3.50
RCCHP	GT	$a^{GT}{}_1$	−0.200
		$a^{GT}{}_2$	0.400
		$a^{GT}{}_3$	0.100
		$b^{GT}{}_1$	−0.101
		$b^{GT}{}_2$	0.202
		$b^{GT}{}_3$	0.458
	GE	$a^{GE}{}_1$	−0.031
		$a^{GE}{}_2$	0.105
		$a^{GE}{}_3$	0.285
		$b^{GE}{}_1$	0.134
		$b^{GE}{}_2$	−0.299
		$b^{GE}{}_3$	0.509
	WT	c_1	−0.010
		c_2	0.317
		c_3	−0.203
		c_4	3.85
	HRSG	COP^{HRSG}	0.900
	EB	COP^{EB}	0.900
	ABS	COP^{ABS}	1.20
	HE	COP^{HE}	0.920
	EC	COP^{EC}	3.50
	ESB	$COP1oss$	0.100
	TST	$COP1oss$	0.100

Table 2
Economic parameters for RCCHP system [6,23,28].

unit		*pi* (¥/kW)
CHP	GT	3800
	GE	4000
WT		8000
PV		9000
GB		370
EB		486
ABS		1944
EC		1512
EBS		4322
TST		200

Table 3
Energy prices for RCCHP system [8,15,30].

	type		price (¥/kWh)
γ	summer	08:00–22:00	1.10
		22:00–08:00	0.540
	other seasons	08:00–22:00	1.06
		22:00–08:00	0.500
λ	GT/GE on-grid		0.360
	PV on-grid		0.770
	WT on-grid		0.540
μ	GT/GE		0.318

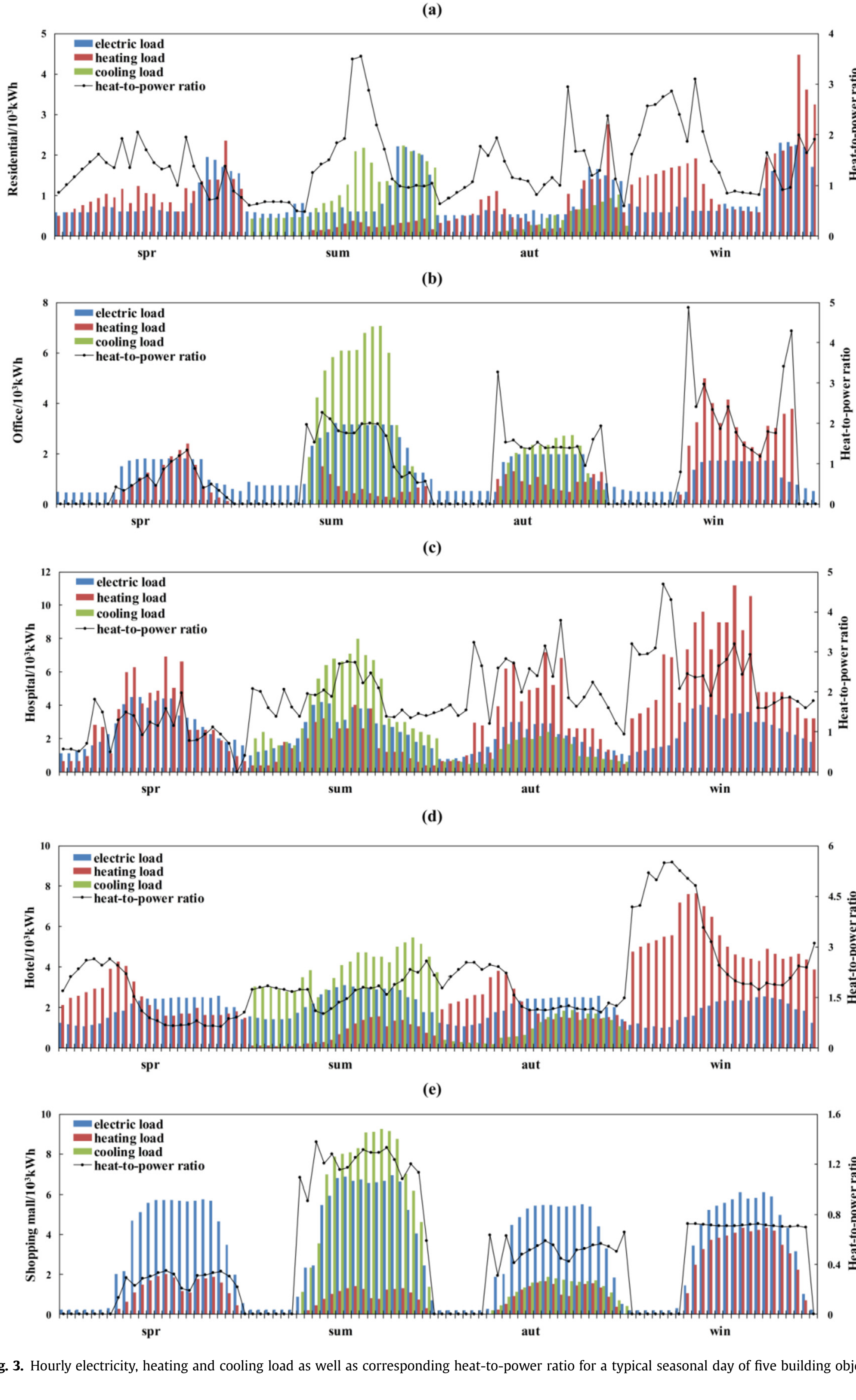

Fig. 3. Hourly electricity, heating and cooling load as well as corresponding heat-to-power ratio for a typical seasonal day of five building objects.

Table 4
The electricity, heating and cooling peak loads of the building: kWh.

	residential	office	hospital	hotel	shopping mall
electricity	2312	3221	4200	3089	6936
heating	4480	4980	11200	7649	4353
cooling	2231	7084	8000	5467	9274

$$HTP_{s,t} = \frac{TL_{s,t} + \left(\frac{CL_{s,t}}{1.2}\right)}{EL_{s,t}} \tag{47}$$

The cumulative frequency of heat-to-power ratio obtained by statistics is shown in Fig. 4(a). In addition, in order to investigate the load characteristics of the building, the mean and standard deviations of the corresponding heat-to-power ratio are shown in Fig. 4(b). Eqs. (48) and (49) show the average ($\overline{HTP}$) and standard (HTP^{stan}) deviations of heat-to-power ratio:

$$\overline{HTP} = \frac{\sum\limits_{s=spr}^{s=win} \sum\limits_{t=1}^{t=24} HTP_{s,t}}{96} \tag{48}$$

$$HTP^{s\ \tan} = \sqrt{\left(\frac{1}{96} \cdot \sum_{s=spr}^{s=win} \sum_{t=1}^{t=24} \left(HTP_{s,t} - \overline{HTP}\right)^2\right)} \tag{49}$$

By entering the above corresponding parameters, a mixed integer nonlinear model is formulated in GAMS software solved by Lindo optimizer with a laptop computer powered by i5 processor and 4 GB of RAM. The time to solve the MINLP model in each building object is less than 15 min.

5.2. Operation results of NOM case

In NOM case, as seen in Fig. 3, residential building has much stable seasonal variation of electrical load for annual basis. As for a typical day, there exists no peak electrical load during daytime while an obvious peak value occurs at night which reaches up to 2 MW. However, the thermal and cooling load of residential building are characterized by much more seasonal variation. The thermal demand at a typical winter day is large and its peak value occurs both at daytime and night when there is hardly any of thermal consumption in a summer day. Similarly, cooling consumption in summer is the major energy load with a peak value both at daytime and night just like winter energy consumption. Therefore, the bigger heat-to-power ratio emerges when cooling and thermal demand is much higher than electricity consumption at summer and winter, respectively. In Fig. 4(a), 64% of the heat-to-power ratio is below 1.5 of residential and the average value is only about 1.42 which is a relatively low level among all five building objects. In general, it is staggered with high fluctuation which matters. On this condition, in residential building, the annual electricity imported from PG decreases from 100% to 12.84% compared to SP system, and the rest 87.16% of the electricity demand are covered by 1.5 MW gas turbine and 4.5 MW wind turbine, as shown in Table 5, accounting for 41.46% and 45.70% respectively. Table 5 displays the design capacity of the technologies allocated in the RCCHP system under NOM and ROM case for five building objects while Fig. 5 shows the percentage of annual electricity, thermal and cooling energy production under NOM and ROM case for five building objects. As shown in Fig. 5(a), the RCCHP system is with significant distinction compared with the single power supply from local PG in the SP system. Fig. 6 shows the hourly electricity combination for a typical summer day under NOM case of five building objects. In a typical summer day, the CHP system and wind turbine cover most electricity demand except for certain time intervals especially during summer night when all the electricity is imported from local PG at an off-peak price. Since it is more economical for summer night with the lower cooling demand at summer nights, it is more economical to import electricity from PG during valley period instead of operating a CHP at lower part load ratio and applying an absorption chiller powered by gradient utilization of waste thermal energy to satisfy cooling load under NOM case. In addition, there is few productions of wind turbine owing to limited wind resource. In Fig. 5(c), all cooling demand of residential at summer nights is covered by electric chiller driven by the electricity imported from PG. Only when there exists peak cooling load at daytime could it implement the combination of absorption chiller and electricity to meet cooling demand. As for operation strategy for winter shown in Fig. 7(a), owing to the desirable wind speed, the electricity production of wind turbine is much more substantial compared with summer, which can better coordinate with CHP to meet the electricity demand of residential, thus dramatically reducing the electricity purchasing from PG. Few electricity consumption is imported from PG except peak load periods at winter nights. The exceed production of wind turbine can access to the local PG pursing optimal economic benefits owing to its high on-grid tariff for 1 kW-hour electricity. In Fig. 8(a) which indicates hourly thermal demand combination for a typical winter day under the NOM case, staggered on-peak hours of heating and electricity load lead to the obvious variations of heat-to-power ratio so that discontinuous operation of the CHP is inevitable. However, the interrupt thermal production can be provided by electric boiler and auxiliary thermal storage tank.

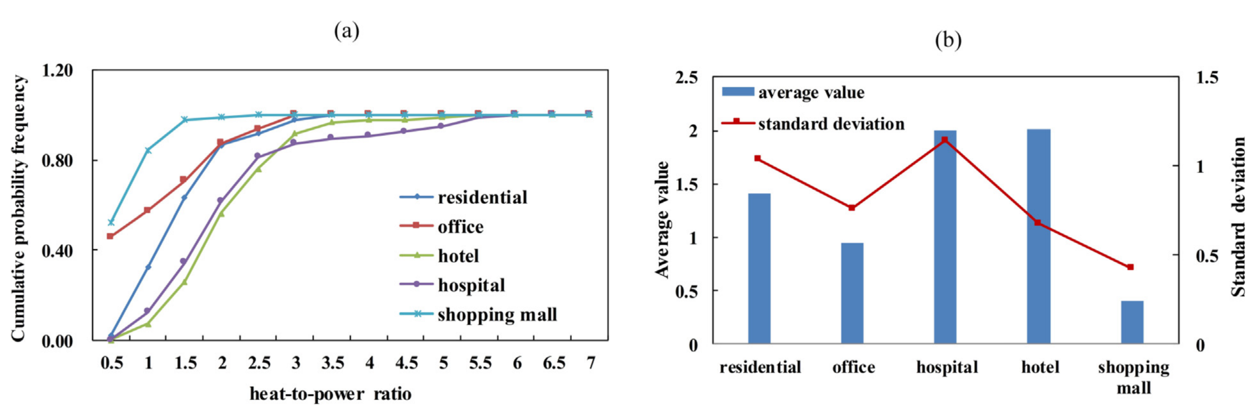

Fig. 4. The cumulative frequency, average value, and standard deviation of heat-to-power ratio of five building objects.

Table 5
The design capacity of technologies allocated in RCCHP system under NPV and IRR optimization for five building objects. (MW).

objective function	building object	technology									
		GT	GE	WT	PV	GB	EB	ABS	EC	EBS	TST
SP system	residential	–	–	–	–	5.0	–	–	3.0	–	–
	office	–	–	–	–	5.0	–	–	7.5	–	–
	hospital	–	–	–	–	12	–	–	8.0	–	–
	hotel	–	–	–	–	8.0	–	–	5.5	–	–
	shopping mall	–	–	–	–	4.5	–	–	9.5	–	–
NPV maximization	residential	1.5	–	4.5	0	–	1.5	2.0	1.0	1.5	1.5
	office	–	3.0	4.5	0	–	4.0	3.0	4.5	2.0	1.5
	hospital	3.6	–	4.5	0	–	9.0	3.5	5.0	2.0	2.0
	hotel	3.0	–	4.5	0	–	5.0	4.0	3.0	2.0	2.0
	shopping mall	–	5.0	4.5	0	–	0.4	4.0	7.5	3.0	3.0
IRR maximization	residential	2.1	–	2.7	0	–	0	2.5	0.8	1.5	1.5
	office	–	5.0	0	0	–	3.0	3.5	4.0	1.5	1.5
	hospital	4.5	–	0	0	–	7.5	4.2	4.5	1.6	2.2
	hotel	4.2	–	0	0	–	3.8	4.8	2.5	1.6	2.5
	shopping mall	–	6.5	0	0	–	1.0	5.6	5.8	2.2	3.2

For office, as indicated in Fig. 5(a), 89% annual electricity consumption is covered by 3 MW gas engine and 4.5 MW wind turbine, accounting for 57% and 31.98%, respectively. Compared with residential, office prefers to choose gas engine with larger capacity as prime mover as well as the same 4.5 MW wind turbine rather than GT. Office is with synchronized on-peak energy demand, as shown in Fig. 3, and it figures in homogeneous heat-to-power ratio with an average value 0.9 which is far below that 1.42 in residential building. What's more, over 71% of heat-to-power ratio is under 1.5. Based on such background, gas engine as prime mover choice which has higher electric efficiency than thermal efficiency is more suitable for office. In addition, as for operation strategy for a summer day shown in Fig. 6(b), gas engine in office keeps operating at the highest and stable part load ratio at daytime from 9 a.m. to 7 p.m. and the rest small amount of electricity is covered by wind turbine production and local PG importation. This is because office is characterized by synchronous on-peak heating and electricity load compared with residential building. In Fig. 7(b) and Fig. 8(b), operation in winter is significantly different from that in summer: Firstly, no purchase from PG is happened even when there occurs a peak load at daytime. GE cooperated with wind turbine and electric storage battery can totally satisfy electricity demand. Secondly, the

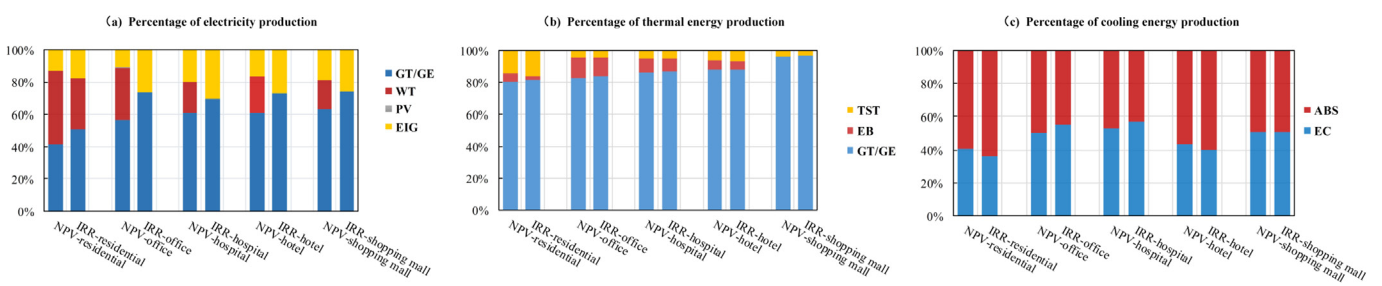

Fig. 5. Percentage of annual electricity, thermal and cooling energy production under NPV and IRR optimization for five building objects.

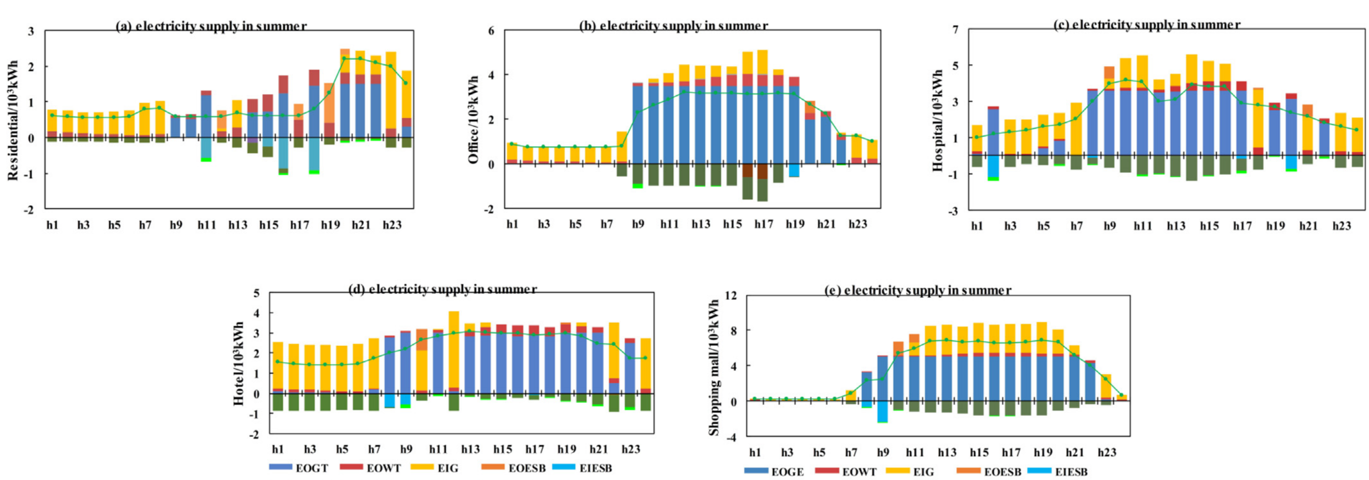

Fig. 6. Hourly electricity combination for a typical summer day under NPV optimization of five building objects.

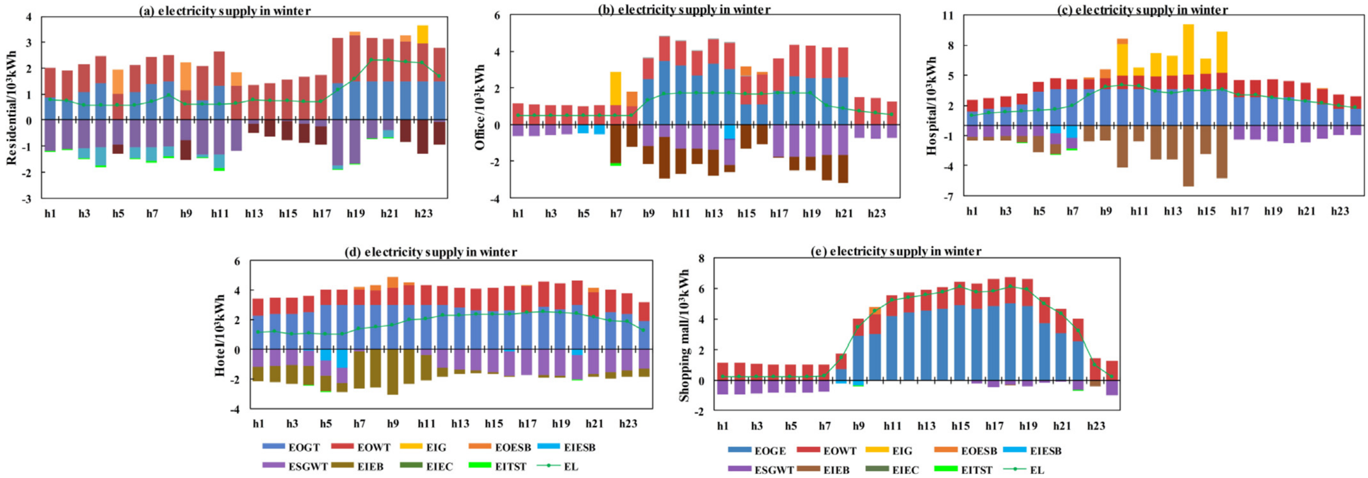

Fig. 7. Hourly electricity combination for a typical winter day under NPV optimization of five building objects.

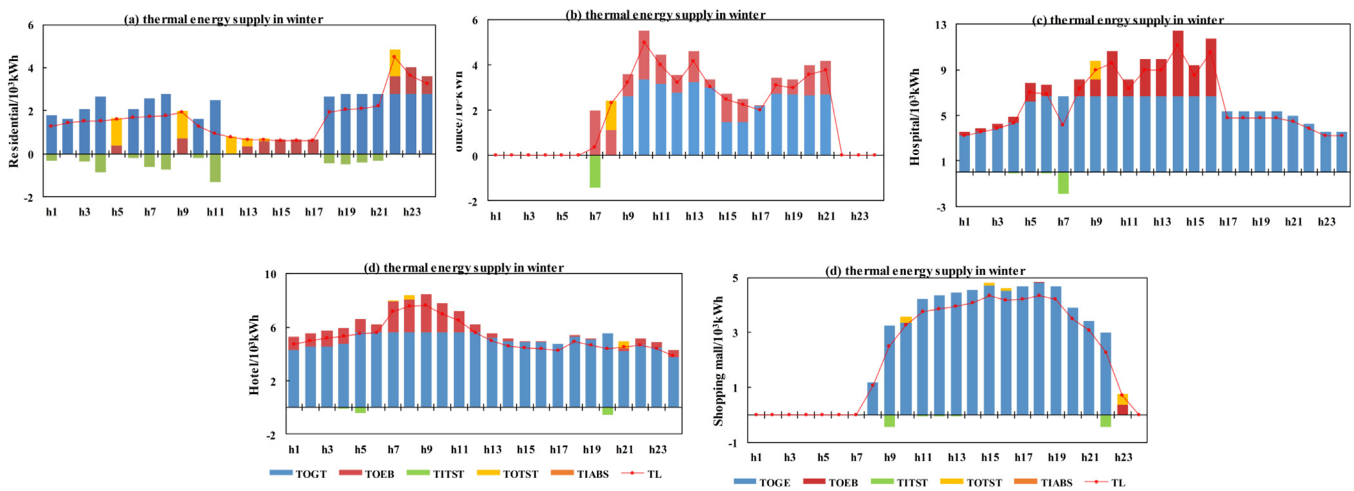

Fig. 8. Hourly thermal demand combination for a typical winter day under NPV optimization of five building objects.

gas engine generation has a certain decrease during time from 3 p.m. to 5 p.m., when the limitation of on-grid wind power is an effective measure to maintain electricity balance. Considering the valley thermal load during this period, energy waste will come up if the gas engine maintains operating in high part load. Thirdly, there is no thermal demand at winter nights so that wind turbine production can completely cover all the electricity requirement and the exceed part can be on-grid at considerable tariff for wind energy regulated by the local government and charge the storage battery. Besides, over 80% of thermal demand is covered by gas engine while the utilization of thermal storage tank shows a certain decrease which is mainly caused by synchronous on-peak heating and electricity load of office, indicating that energy storage system is more suitable for such a terminal like residential building with complex energy demand.

For Hospital, compared with the above two buildings, the biggest change is that the chosen 4.5 MW wind turbine has a significant decrease in power production to 19.84% but gas turbine accounts for over 60% of annual electricity consumption. What results in this situation is hospital features overall high level of energy demand which has synchronous on-peak hours of heating and electricity load. Obviously, it is favorable for the CHP to maintain a high part load generation with excellent efficiency. As seen in Fig. 4, over 54% of heat-to-power ratio in hospital is between 1.5 and 3, and the average value is almost 2. Hospital prefers to gas turbine with a big capacity as a prime mover, which has larger thermal energy production than electricity. Compared with office, there is still continuous small amount of cooling demand at summer nights of hospital. Therefore, importation from local PG at valley price cooperated with electric chiller to generate cooling energy instead of operating CHP with lower part load radio is rather economic operation strategy for hospital. However, as for the RCCHP system operation in winter, difference from the above two building system is that although CHP can operate 24 h with relative high part load ratio to provide energy demand, it is unable to cover peak energy demand completely and much more supplementary electric boiler is necessary to produce exceed energy. In this case, electricity imported from PG at 10a.m.-16p.m. is necessary even when there is non-trough price charge. As illustrated in Fig. 5(a), electricity purchasing proportion of hospital is much higher than that of the aforementioned buildings, reaching up to 19.85%.

According to Figs. 4 and 5, three types of energy demands of hotel are rather similar with those of hospital. The fluctuation of energy load is stable and heat-to-power ratio turns out to be totally high. In terms of electricity combination, the significant distinction compared with hospital is none peak electricity value existing in winter of hotel which is to the benefit of capacity allocation of gas turbine as well as maintaining its high operation efficiency. Besides, no electricity is imported from PG so that the percentage of annual electricity consumption from PG of hotel has decrease from 19.85% to 16.65% compared with that of hospital shown in Fig. 5(a). For thermal and cooling operation, similarly, owing to relatively slighter fluctuation of thermal and cooling demand compared with hospital, the energy production proportion of gas turbine and electric chiller has been improved to some degree. As consequence, the contribution of supplementary electric chiller and electric boiler has been limited.

For shopping mall, which has the lowest heat-to-power ratio performance shown in Fig. 4, almost 98% of heat-to-power ratio is below 1.5, and the average value is as low as 0.4, which implies that shopping mall needs more electricity than thermal (cooling) demand. On this condition, a 5 MW gas engine and a 4.5 MW wind turbine are chosen in shopping mall RCCHP systems, which cover 60% and 17.23% of total annual electricity demand, respectively, and the rest 17.77% is imported from local PG. Compared with office, the shopping mall has an even lower heat-to-power ratio due to the decreased electricity demand in a summer night. Nevertheless, there is an increased demand on PG electricity. Because a lower heat-to-power ratio (especially at winter days) would weaken the influence of maximum thermal load on the optimal capacity decision of CHP, thus a relative smaller size of CHP would be more suitable for shopping malls, resulting in more electricity imported from PG. As for the electricity and cooling demand, the electricity demand that exceeds CHP generation can be supplied by PG or wind turbine, which is more for satisfying electricity demand rather than on-grid revenue in shopping mall and the insufficient cooling energy could be supplemented by the auxiliary electric chiller generation. Hardly any energy demand at nights is required for shopping mall, and during daytime the slight fluctuation of energy load curve drives CHP operating at relatively high part load ratio. Although the initial investment cost of a shopping mall is the largest of all five construction projects, its dynamic payback period is the shortest. On the contrary, residential building features staggered on-peak hours of heating and electricity load which result in complex operation condition for the RCCHP system. Therefore, even the RCCHP in residential building is designed with the least initial investment cost, the system still has a long dynamic payback period.

5.3. Operation results of ROM case

NOM case is an option for decision makers who focus on system sizing and long-term economic benefits while it also means a higher initial investment cost. However, when it comes to optimizing return of unit capital cost as well as the shortest dynamic payback period, ROM case performs better. The performance indexes under NOM and ROM cases for five building objects are shown in Table 6. As indicated in Table 6, in ROM case, the DPP and NPV decrease evidently along with the limited GSR and CER as well. However, electricity from PG increases oppositely. What's more, the utilization of wind turbine and electric storage battery is limited under ROM case due to its high capital cost, which means that the larger investment boosts long-term benefits while the shortest DPP pursuing is against the economic and environmental benefits in

Table 6
The performance indexes under NPV and IRR optimization for five building objects.

objective function	building object	performance index						
		NPV(¥ million)	IRR(%)	DPP(year)	IIC(¥ million)	GSR(%)	CER(%)	EUR(%)
NPV maximization	residential	8.790	8.700	8.93	55.30	37.98	47.71	66.70
	office	25.84	13.20	7.24	69.55	35.90	42.10	67.41
	hospital	37.41	15.20	6.71	78.15	31.30	36.20	72.50
	hotel	33.53	14.70	6.82	71.88	36.14	38.70	65.41
	shopping mall	67.75	20.70	5.49	90.32	33.87	32.70	64.30
IRR maximization	residential	7.260	9.400	8.63	40.63	16.25	42.61	68.23
	office	12.84	14.90	6.76	32.87	13.82	30.32	58.65
	hospital	22.84	17.90	6.03	41.46	13.73	27.15	65.39
	hotel	20.15	17.60	6.09	35.19	14.22	30.93	60.90
	shopping mall	46.41	25.10	4.82	53.63	14.57	25.34	59.73

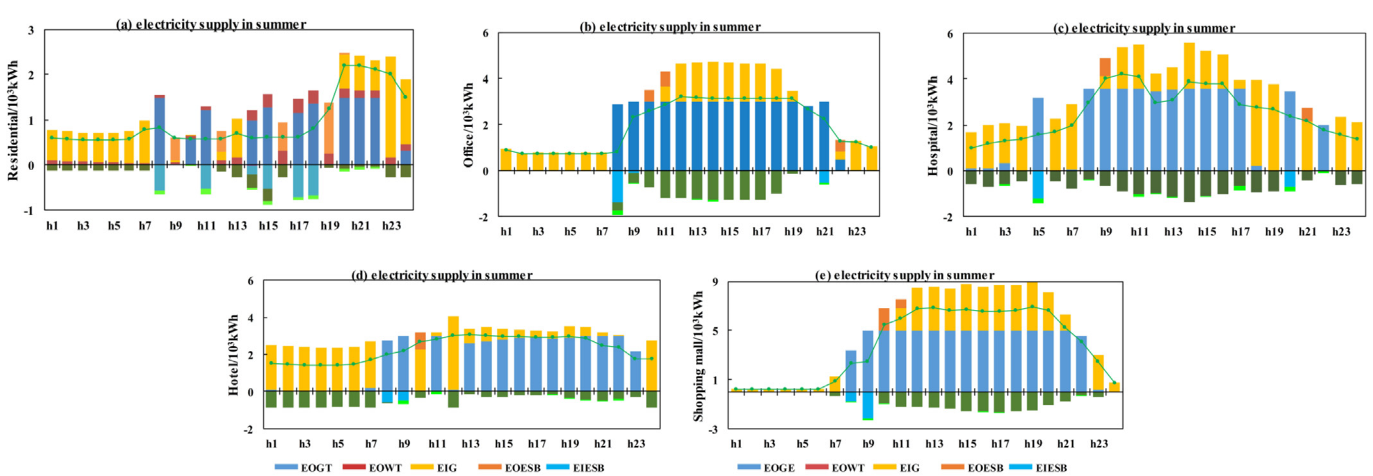

Fig. 9. Hourly electricity combination for a typical summer day under IRR optimization of five building objects.

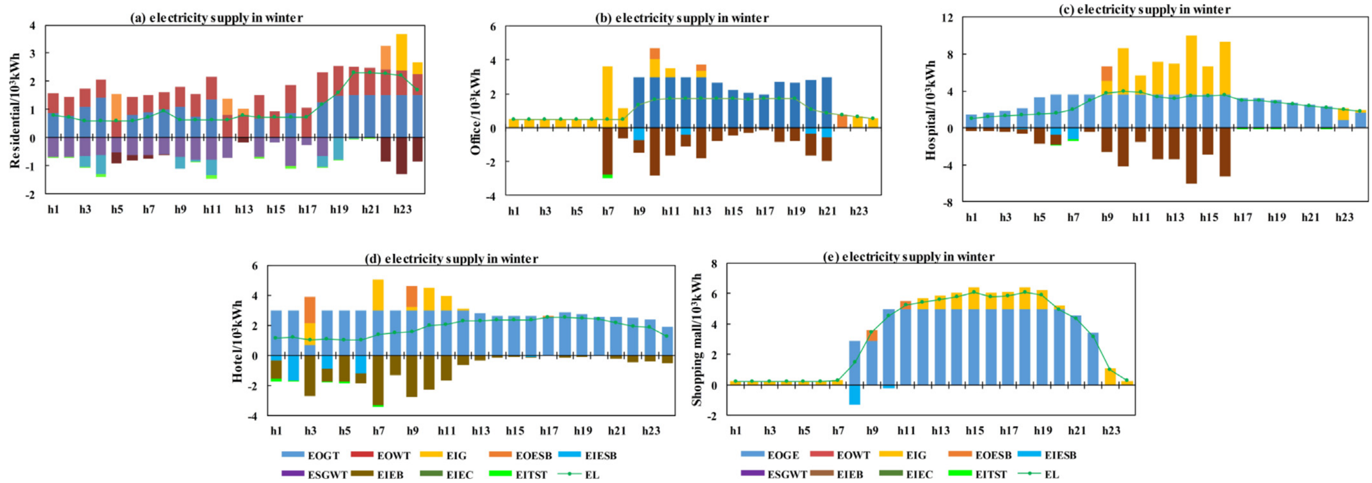

Fig. 10. Hourly electricity combination for a typical winter day under IRR optimization of five building objects.

some degree. In other words, there is a trade-off between the shortest DPP and long-term benefits.

As for the electricity supply combination illustrated in Fig. 9, compared with NOM case, there is no change in the selection of prime mover type for all five building objects. However, the installed capacity has been significantly improved. Wind turbine is adopted only in residential building, which indicates that the adoption of wind turbine in buildings with large scale load fluctuations yields better economic and environmental benefits and has the shortest payback period in the long term. Furthermore, gas turbine in residential building is not able to maintain stable operation due to its staggered load distribution. In spite of the high investment cost, wind turbine as complementary power production can effectively coordinate energy supply in staggered on-peak hours associated with decreasing the investment cost of prime mover and its incremental O&M cost as a consequence of lower part load operation condition. Above all, as reflected by operation combination for a typical winter day shown in Fig. 10, electricity imported from PG increases observably especially during off-peak night for all building system except residential building. More electricity from local PG to satisfy the electricity demand improves the speed of cost recovery. In the long term, NPV of all five buildings under ROM case has a marked decline. It is worth mentioning that although the power storage equipment has little capacity change under ROM case compared with NPV optimization, it obviously increases in the operating frequency, indicating that the electricity storage battery plays an important role in dispatching the peak-valley power demand. However, the large-scale deployment of power storage equipment has been limited due to its high price.

As for cooling load, the installed capacity of absorption chiller increases due to the increased installed capacity of CHP under ROM case, while the installed capacity of electric chiller decreases slightly. However, the output composition changes little in terms of summer cooling load, with absorption chiller playing as the main source of energy production supplemented by electric chiller. Similarly, gas turbine or gas engine undertakes most thermal energy supply in winter days and the utilization of electric boiler is limited obviously. For example, electric boiler is obviously not a desirable choice taking part in energy balance at 12 a.m.-5 p.m. in residential building or 3 p.m.–4 p.m. in office. Hourly thermal load combination for a typical winter day under ROM case is shown in Fig. 11. However, the utilization of thermal storage tank in Fig. 11 becomes more frequent especially at off-peak load period, which illustrates that thermal storage is an effective setting to avoid CHP operating with a much lower part load ratio inefficiently. In office, large amount of thermal energy is charged in thermal tank at 7 a.m.

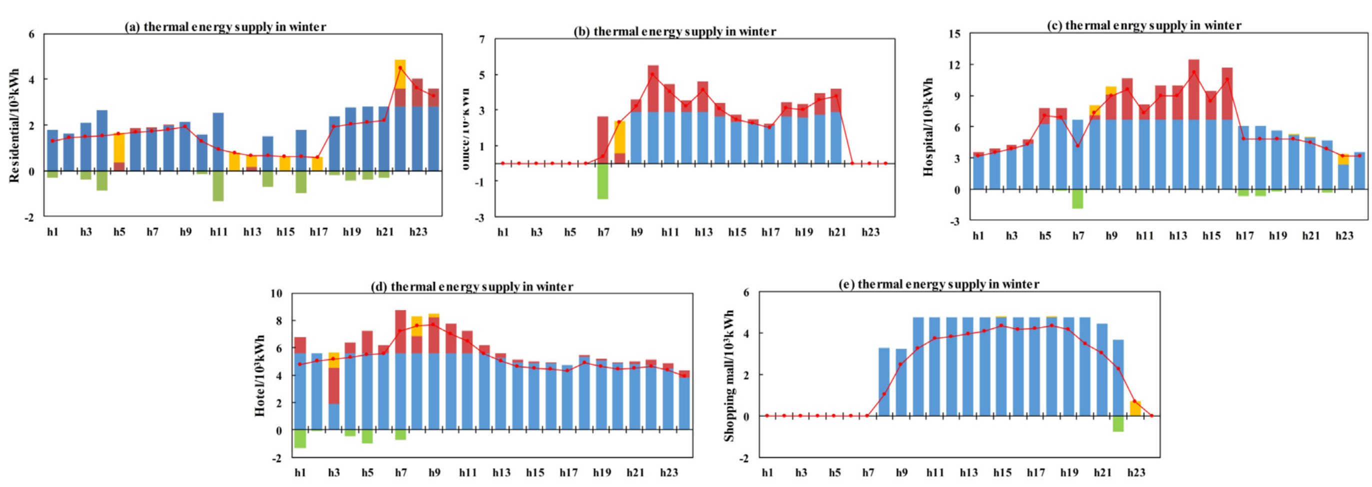

Fig. 11. Hourly thermal load combination for a typical winter day under IRR optimization of five building objects.

and discharged at 8 a.m. when thermal demand increases much more than electricity consumption, otherwise the gas engine operation may lead to electricity waste. In addition, more thermal energy storage discharges at 8 a.m. instead of operating an electric boiler compared with NPV optimization, which illustrates that thermal storage tank has a greater advantage of price over electric boiler in recovering investment under the premise of satisfying thermal energy demand.

Considering both economic and environmental benefits, the RCCHP system has notable success in achieving peak shaving and valley filling for energy demand of all building objects compared with SP system no matter under NOM or ROM case. The dynamic payback period under IRR optimization is much lower than that under NOM case. Compared with GSRs and CERs of five buildings under NOM and ROM optimizations, GSRs under ROM optimization has decreased 17.57%–22.08% while CERs under ROM optimization has decreased about 5.1%–11.78%. It is sure that IRR maximum project obtains worse performance from long-term aspect. Obviously, optimized results under NOM case show that the RCCHP system for all the buildings are scaled up larger than that under ROM case and from long-term economic and environmental aspect, NOM case has greater advantage. Although the simple pursuit of the maximum IRR results in initial investment cost reduction compared with NOM case, it fails to realize the desirable system size for long-term benefits.

6. Conclusions

This research builds a RCCHP system consisting of the CHP subsystem, renewable energy subsystem, auxiliary heating and cooling subsystem as well as energy storage subsystem to optimize the energy combination of valley-peak load for energy demand terminal. NOM and ROM cases are introduced and applied in five common buildings for cost saving and exploring the hourly dispatch, demand side management potential and energy technology applicability. Some conclusions are summarized as follows.

Firstly, optimal capacity of technology combination under NOM case, as with the incremental initial investment cost, is much larger than that under ROM case with better energy self-sufficiency. At the same time, wind turbine is chosen only in the residential building under ROM case, hence the incremental electricity imported from power grid is necessary, which is definitely obstruction for pursuing long-term economic benefits and environmental performance, while it's worth noting that energy storage operates much frequently in ROM case.

Secondly, compared with SP system, economic benefits of RCCHP system application for the five common building objects have substantial improvement. NPV and IRR values reach up to 67.75 million RMB and 25.10% under NOM and ROM case for shopping mall, and the shortest DPP is 4.82 years under ROM case. Besides, as the results of optimization, the values of GSR and CER perform excellent, reaching up to 37.98% and 47.71%, respectively. From the point of NPV and IRR evaluation, shopping mall > hospital > hotel > office > residential building.

Thirdly, building objects characterized with corresponding high level of heat-to-power ratio are mainly supplied by gas turbine, while those features with more electricity demand than thermal consumption are more likely to adopt gas engine.

Fourthly, wind turbine plays a more critical role on buildings which feature fluctuated energy demand, which is because dynamic efficiency by curve fitting is of use in prime mover, thus wind turbine can keep CHP running at a high load level effectively, decrease the operation cost, reduce the maximum installed capacity of CHP, cut power purchase from public grid, as well as achieve better economic and environmental benefits.

Acknowledgements

The authors are grateful for the support from National Natural Science Foundation of China under grant No. 51876181. The work is also supported by the Science and Technology Planning Projects of Fujian Province, China with grant No. 2018H0036.

Nomenclature

A	average size of a PV panel
a	fitted coefficient for electric efficiency
b	fitted coefficient for thermal efficiency
c	fitted coefficient for wind power curve
CE	carbon emission
CER	carbon emission reduction rate
CL	cooling load
CO	output cooling energy
COP	coefficient of performance
COPel	electrical coefficient of performance for prime mover
COPth	thermal coefficient of performance for prime mover
CR	rated power for cooling technologies
Cut	cut-out coefficient
E	electricity storage energy
EI	input electricity
EIG	electricity imported from Grid
EL	electrical load
ELS	electricity loss
EO	output electricity
ER	rated power for electric technologies
ES	electricity surplus
ESG	electricity sold back to Grid
EUR	energy utilization rate
F	part load factor
GSR	gas saving rate
GC	gas consumption
HTP	heat-to-power ratio
$\overline{HTP}$	average value of *HTP*
i	discount rate
IIC	initial investment cost
IRR	internal rate of return
NG	natural gas
NPV	net present value
Num	allocated number
Pi	unit investment cost factor
Pm	unit maintain cost factor
SC	annual cost saving
Th	thermal storage energy
T	whole time horizon
TA	available allocated space
TI	input thermal energy
TL	thermal load
TLS	thermal energy loss
TO	output thermal energy
TOC	total operation cost
TR	rated capacity for thermal technologies
v	wind speed
w	time-related solar irradiation
x	binary variable

Greek letters

α	carbon emission factor
γ	time-of-use electricity price
λ	electricity feed-in tariff
μ	natural gas price

φ carbon tax

Subscript

c	technology
cc	cooling technology
ec	electric technology (i.e. power generator)
m	number of prime mover
s	season
t	hour
tc	thermal technology
y	year

Superscript

ABS	absorption chiller
CCHP	combined cooling heating and power system
CHP	combined heating and power
EB	electric boiler
EC	electric chiller
el	electricity
ESB	electricity storage battery
GE	gas engine
GT	gas turbine
HE	heat exchanger
HRSG	heat recovery steam generator
in	cut in
ng	natural gas
out	cut out
PG	power grid
PV	photovoltaic
rated	rated
RCCHP	combined cooling heating and power system coupled with renewable energy
SP	separate production
stan	standard deviation
TST	thermal storage tank
WT	wind turbine

References

[1] C. Delmastro, E. Lavagno, G. Mutani, Chinese residential energy demand: scenarios to 2030 and policies implication, Energy Build. 89 (2015) 49–60.

[2] E. Mehleri, H. Sarimveis, N. Markatos, Optimal design and operation of distributed energy systems: application to Greek residential sector, Renew. Energy 51 (2013) 331–342.

[3] A. Mosaffa, L. Farshi, Thermodynamic and economic assessments of a novel CCHP cycle utilizing low-temperature heat sources for domestic applications, Renew. Energy 120 (2018) 134–150.

[4] T. Wakui, K. Sawada, H. Kawayoshi, et al., Optimal operations management of residential energy supply networks with power and heat interchanges, Energy Build. 151 (2017) 167–186.

[5] W. Stanek, W. Gazda, W. Kostowski, et al., Thermo-ecological assessment of CCHP (combined cold-heat-and-power) plant supported with renewable energy, Energy 92 (2015) 279–289.

[6] M. Liu, Y. Shi, F. Fang, et al., A new operation strategy for CCHP systems with hybrid chillers, Appl. Energy 95 (2012) 164–173.

[7] M. Farahnak, M. Gord, F. Dashti, et al., Optimal sizing of power generation unit capacity in ICE-driven CCHP systems for various residential sizes, Appl. Energy 158 (2015) 203–219.

[8] X. Luo, K. Fong, Development of multi-supply-multi-demand control strategy for combined cooling, heating and power system primed with solid oxide fuel cell-gas turbine, Energy Convers. Manag. 154 (2017) 538–561.

[9] H. Rahman, M. Majid, A. Jordehi, Operation and control strategies of integrated distributed energy resources: a review, Renew. Sustain. Energy Rev. 51 (2015) 1412–1420.

[10] S. Sepehr, K. Navid, Simultaneous use of MRM (maximum rectangle method) and optimization methods in determining nominal capacity of gas engines in CCHP (combined cooling, heating and power) systems, Energy 72 (2014) 145–158.

[11] J. Wu, J. Wang, S. Li, Experimental and simulative investigation of a micro-CCHP (micro combined cooling, heating and power) system with thermal management controller, Energy 68 (2014) 443–453.

[12] A. Facci, L. Andreassi, S. Ubertini, Optimization of CHCP (combined heat power and cooling) systems operation strategy using dynamic programming, Energy 66 (2014) 387–400.

[13] X. Teng, X. Wang, Y. Chen, et al., A simple method to determine the optimal gas turbine capacity and operating strategy in building cooling, heating and power system, Energy Build. 80 (2014) 623–630.

[14] G. Yang, C. Zheng, X. Zhai, Influence analysis of building energy demands on the optimal design and performance of CCHP system by using statistical analysis, Energy Build. 153 (2017) 297–316.

[15] I. Askari, M. Sadegh, M. Ameri, et al., Effect of heat storage and fuel price on energy management and economics of micro CCHP CHP systems, Mech. Sci. Technol. 28 (5) (2014) 2003–2014.

[16] X. Chen, Y. Wang, H. Yu, et al., A domestic CHP system with hybrid electrical energy storage, Energy Build. 55 (2012) 361–368.

[17] D. Xu, M. Qu, Energy, environmental, and economic evaluation of a CCHP system for a data center based on operational data, Energy Build. 67 (2013) 176–186.

[18] R. Zeng, H. Li, A novel method based on multi-population genetic algorithm for CCHP–GSHP coupling system optimization, Energy Convers. Manag. 105 (2018) 1138–1148.

[19] M. Li, X. Jiang, D. Zheng, Thermodynamic boundaries of energy saving in conventional CCHP (Combined Cooling, Heating and Power) systems, Energy 94 (2016) 243–249.

[20] X. Jiang, D. Zheng, Y. Mi, et al., Carbon footprint analysis of a combined cooling heating and power system, Energy Convers. Manag. 103 (2015) 36–42.

[21] P. Mago, L. Chamra, Analysis and optimization of CCHP systems based on energy, economical, and environmental considerations, Energy Build. 41 (10) (2009) 1099–1106.

[22] M. Somma, G. Graditi, E. Heydarian-Forushani, et al., Stochastic optimal scheduling of distributed energy resources with renewables considering economic and environmental aspects, Renew. Energy 116 (2018) 272–287.

[23] D. McLarty, J. Brouwer, C. Ainscough, Economic analysis of fuel cell installations at commercial buildings including regional pricing and complementary technologies, Energy Build. 113 (2016) 112–122.

[24] D. Maraver, A. Sin, F. Sebasti, et al., Environmental assessment of CCHP (combined cooling heating and power) systems based on biomass combustion in comparison to conventional generation, Energy 57 (2013) 17–23.

[25] A. Rong, Y. Su, Polygeneration systems in buildings: a survey on optimization approaches, Energy Build. 151 (2017) 439–454.

[26] A.H. Nosrat, L.G. Swan, J.M. Pearce, Improved performance of hybrid photovoltaic-trigeneration systems over photovoltaic-cogen systems including effects of battery storage, Energy 49 (2013) 366–374.

[27] H. Cho, P.J. Mago, R. Luck, et al., Evaluation of CCHP systems performance based on operational cost, primary energy consumption, and carbon dioxide emission by utilizing an optimal operation scheme, Appl. Energy 86 (12) (2009) 2540–2549.

[28] Z. Wang, W. Han, N. Zhang, et al., Proposal and assessment of a new CCHP system integrating gas turbine and heat-driven cooling/power CHP, Energy Convers. Manag. 144 (2017) 1–9.

[29] F. Jabari, S. Nojavan, B. Mohammadi Ivatloo, et al., Optimal short-term scheduling of a novel tri-generation system in the presence of demand response programs and battery storage system, Energy Convers. Manag. 122 (2016) 95–108.

[30] A. Moaleman, A. Kasaeian, M. Aramesh, et al., Simulation of the performance of a solar concentrating photovoltaic-thermal collector, applied in a combined cooling heating and power generation system, Energy Convers. Manag. 160 (2018) 191–208.